Published in final edited form as:
Nature. 2008 December 11; 456(7223): 745–749. doi:10.1038/nature07525.

Brain metabolic state dictates the polarity of astrocyte control over the cerebrovasculature

Grant R. J. Gordon[1], **Hyun Beom Choi**[1], **Graham C. R. Ellis-Davies**[2], and **Brian A. MacVicar**[1,*]

[1]Brain Research Centre,Department of Psychiatry, University of British Columbia, BC, Canada

[2]Department of Pharmacology & Physiology, Drexel University College of Medicine, Philadelphia, Pennsylvania, USA

Abstract

Calcium signaling in astrocytes couples changes in brain activity to regional alterations in cerebral blood flow (CBF) by eliciting vasoconstriction or vasodilation of adjacent arterioles[1-7]. However, the mechanism for how these disparate astrocyte influences provide appropriate changes in cerebral vascular tone within a cellular environment that has dynamic metabolic requirements remains unclear. The regulation of CBF has recently been shown to be tightly coupled to the lactate/pyruvate ratio and thus the NADH/NAD^+ ratio in animals[8] and humans[9,10]. We tested the impact of metabolic changes on the regulation of cerebral blood vessel diameter by astrocytes, by manipulating tissue oxygenation which changes dynamically with brain activity[11-14]. Using two-photon Ca^{2+} imaging and uncaging as well as intrinsic nicotinamide adenine dinucleotide (NADH) imaging of single cells as a measure of redox state, we show that the ability of astrocytes to induce vasodilations over vasoconstrictions critically relies on the metabolic state of the tissue. When O_2 availability is lowered and astrocyte $[Ca^{2+}]_i$ is elevated, astrocyte glycolysis and lactate release are maximized. Extracellular lactate contributes to prostaglandin E_2 (PGE_2) accumulation by hindering its transporter-mediated uptake, subsequently causing vasodilation. These data reveal the role of metabolic substrates in regulating CBF and provide a mechanism for differential astrocyte control over cerebrovascular diameter during different states of brain activation.

We first examined whether changing PO_2 consistently determined whether vasoconstrictions or vasodilations were evoked by astrocyte Ca^{2+} transients. The mGluR agonist t-ACPD (100 μM) potently increased $[Ca^{2+}]_i$ (240.0 ± 19.1 %, n = 14, $P < 0.01$, Fig. 1 a) in astrocytes[1,4,5] and differential responses were observed in the adjacent cerebral blood vessels whereby vasodilation (107.0 ± 0.8 % (100% = control diameter), $P < 0.01$, n = 23, Fig. 1 a, d) occurred in low O_2 but in high O_2 arterioles constricted[1] (85.4 ± 4.0 %, $P < 0.01$, n = 10, Fig. 1 d). We next used two-photon photolysis of the Ca^{2+} cage DMNPE-4[15] to examine the

*Correspondence T: 604-822-7797, F: 604-822-7299, bmacvicar@brain.ubc.ca.

Author Contributions G.R.J.G. and B.A.M. designed the imaging experiments and wrote the manuscript. G.R.J.G. performed the imaging experiments and analysis and took slice PO2 measurements. H.B.C., G.R.J.G. and B.A.M. designed the lactate and PGE2 experiments. H.B.C. and B.A.M. designed the immunohistochemistry experiments. H.B.C. performed the lactate and PGE_2 measurements and analysis and the immunohistochemistry. G.C.R.E-D designed and synthesized the calcium cage. All authors helped edit the manuscript.

effect of low O_2 levels on the impact of directly evoked astrocyte Ca^{2+} signals on adjacent blood vessels. Uncaging DMNPE-4 triggered Ca^{2+} waves that spread to multiple endfeet circumscribing arterioles (Fig. 1 b, c). In contrast to previous results in high PO_2 where Ca^{2+} transients in astrocyte endfeet always caused constriction[1], in low O_2 endfeet Ca^{2+} (232.2 ± 8.5 %, n = 17, $P < 0.01$) caused arteriole dilations (107.4 ± 1.0 %, $P < 0.01$, n = 17, Fig. 1 b, c, d) that were repeatable (Fig. 1 b). The Ca^{2+} change preceded the enlargement of lumen diameter (Fig. 1 b, c). These data suggest PO_2 dictates the polarity of the change in arteriole diameter caused by either mGluR activity or an elevation in endfoot Ca^{2+} and that the dilation process can be initiated solely by astrocyte activation (see Supplemental Fig. 1 for PO_2 measurements). Ca^{2+} activates $cPLA_2$ triggering arachidonic acid (AA) formation that is either converted to 20-HETE[1] in (SMCs) causing vasoconstriction or is converted to the vasodilator PGE_2 in astrocytes via cyclooxygenase (COX) enzymes[4,7]. We confirmed COX expression in astrocytes and their endfeet (Supplemental Fig. 2). The COX inhibitor indomethacin (100 μM) blocked vasodilations caused by t-ACPD (98.4 ± 0.8 %, $P > 0.05$, n = 9, Fig. 1 d) and by caged Ca^{2+} photolysis (101.0 ± 0.5 %, $P > 0.05$, n = 6, Fig. 1 d) in low O_2. Application of the COX product PGE_2 (1 μM) elicited vasodilation (109.4 ± 2.7 %, $P < 0.05$, n = 4, Fig. 1 d), confirming COX activation and the generation of PGE_2 is an important signaling molecule in astrocyte-mediated vasodilations in low O_2[4,7].

Next we examined how changing tissue PO_2 could modify whether astrocyte Ca^{2+} transients induce constrictions versus dilations. We examined the possibility that a lower PO_2 elevates anaerobic metabolism, increasing external lactate which subsequently enhances external PGE_2 concentrations. Once produced, PGE_2 passively diffuses into the extracellular space[16] and its action on smooth muscle cells is terminated when prostaglandin transporters (PGTs) take up PGE_2 by an exchange of intracellular lactate[17]. Due to the influence of a lactate concentration gradient on PGT efficacy, we tested the hypothesis that higher levels of extracellular lactate reduce the ability of PGT to uptake PGE_2[17] from the extracellular space, thereby increasing PGE_2 concentrations resulting in vasodilation. Such a role for lactate is consistent with the observations that extracellular lactate levels increase immediately during brain activity[18] and that lactate is known to enhance activity dependent increases in blood flow[8]. We found using immuohistochemistry that PGT is widely expressed in brain grey matter in both astrocyte endfeet (Fig. 2 a), and neurons (Fig. 2 b), indicating dendrites as well as endfeet take up prostaglandins. Consistent with a positive correlation between external lactate and PGE_2, we found that low O_2 enhanced lactate release from brain slices (low: 114.2 ± 9.1 μM, n = 6; high: 41.9 ± 5.6 μM, n = 6, $P < 0.01$, Fig. 2 c). Also, significantly greater levels of PGE_2 were observed in low O_2 when PGE_2 production was triggered by mGluR activation, (low: 136.1 ± 10.2 pg/ml, n = 6; high: 91.9 ± 12.6 pg/ml, n = 4, $P < 0.01$, Fig. 2 d). Furthermore, addition of lactate (1 mM) enhanced the PGE_2 level (control: 40.5 ± 3.3 pg/ml; + lactate: 58.0 ± 3.1 pg/ml, n = 5, $P < 0.01$) and increased arteriole diameter (107.5 ± 1.0 %, $P < 0.01$, n = 15, Fig. 2 e, f, g). Dilations induced by lactate were blocked by indomethacin (100.4 ± 0.4 %, $P > 0.05$, n = 11, Fig. 2 g) indicating they were mediated by PGE_2. These data indicate that in low O_2 the higher level of extracellular lactate raises external levels of PGE_2. This is consistent with lactate reducing PGE_2 uptake through PGT.

We next examined the role of glycolysis in lactate production by imaging the intrinsic fluorescence of the metabolic electron carrier NADH in astrocytes. Two-photon excitation of NADH provides a sensitive, subcellular measure of both oxidative metabolism (punctate NADH fluorescence from mitochondria) and glycolytic metabolism (diffuse NADH fluorescence from the cytosol)[19]. We observed, as previously reported, that astrocytes (stained with SR-101[20]) showed bright intracellularly diffuse NADH fluorescence in the soma and endfeet (Fig. 2 h, i). Stimulating glycolysis with low O_2 increased the astrocyte NADH signal (124.6 ± 1.4 %, n = 7, $P < 0.01$, Fig. 2 i, j) and inhibiting glycolysis with iodoacetate (IA, 200 μM) reduced basal NADH fluorescence (87.8 ± 2.0 %, n = 5, $P < 0.05$, Fig. 2 k). Furthermore, inhibiting lactate dehydrogenase (LDH) (which converts pyruvate and NADH to lactate and NAD+; see Fig. 4 e diagram) with oxamate (2.5 mM) increased the NADH signal (119.3 ± 2.0 %, n = 6, $P < 0.01$, Fig. 2 l). These data support the conclusion that NADH is generated to a significant extent in astrocytes as a consequence of glycolytic metabolism—likely originating from glycogen breakdown[21]—which can be augmented by reducing O_2.

Recent two-photon NADH imaging demonstrated an increase in astrocyte glycolysis subsequent to the onset of neuronal activity[19]. We hypothesized that mGluR activation further enhances glycolysis in astrocytes in low O_2, promoting greater extracellular lactate levels that cause vasodilation. Consistent with this idea, t-ACPD enhanced extracellular lactate, which was greatest in low O_2 (low: 186.7 ± 11.2 μM, n = 6; high: 98.6 ± 10.2 μM, n = 7, $P < 0.01$, Fig. 3 f). The astrocytes were a site of increased glycolysis because t-ACPD triggered an increase in cytosolic NADH (128.7 ± 4.1 %, n = 7, $P < 0.01$, Fig. 3 a, b, c, d, e) coincident with lumen widening (108.5 ± 0.7 %, n = 5 of 7, $P < 0.01$, Fig. 3 b, c). In contrast, peak NADH signals from perivascular neurons were not as great and were qualitatively different, showing distinct punctate mitochondrial fluorescence (Supplemental Fig. 3). These data signify a change in anaerobic metabolism may be important for astrocyte-mediated vasomotion in low O_2.

Recent functional imaging data from human subjects reveals a relationship between a rise in the lactate/pyruvate and thus NADH/NAD^+ ratios and an increase in CBF[9], but how this enhanced glycolytic state is a critical step translating information on the level of brain activity into vasodilation of arterioles is not known. Our data demonstrate that lactate, astrocyte NADH and PGE_2 are maximally increased in low O_2 when mGluRs are activated and that exogenous lactate can mediate prostaglandin dependent vasodilation. Therefore, we tested the hypothesis that glycolysis and thus lactate production is essential for prostaglandin dependent astrocyte-mediated vasodilations. We used two separate pharmacological treatments to limit the lactate released by mGluR activity in low O_2. First, in the presence of IA to block the source of lactate, t-ACPD instead decreased astrocyte NADH (81 ± 0.4 %, n = 5, $P < 0.01$, Fig. 3 g) and failed to dilate vessels (97.8 ± 0.2 %, n = 5, $P > 0.05$, Fig. 3 i). Second, in the presence of oxamate to curtail lactate formation, t-ACPD still increased astrocyte NADH (113.8 ± 3.1 %, n = 6, $P < 0.05$, Fig. 3 h)—an expected outcome as oxamate acts downstream of NADH production (see Fig. 4 c diagram)—yet vasodilations no longer occurred (99.0 ± 0.1 %, n = 6, $P > 0.05$, Fig. 3 i). We then confirmed the lack of vasomotion observed during these treatments was associated with a significant reduction in

lactate and PGE_2 release when mGluRs were activated (Lactate release in t-ACPD: 180.2 ± 11.9 μM, n = 6; + IA: 88.2 ± 8.8 μM, n = 6, $P < 0.01$; + Oxamate: 89.1 ± 6.6 μM, n = 6, $P < 0.01$, Fig. 3 j)(PGE_2 release in t-ACPD: 154.0 ± 10.1 pg/ml, n = 4; + IA: 115.4 ± 10.6 pg/ml, n = 6, $P < 0.01$; + Oxamate: 94.6 ± 7.6 pg/ml, n = 6, $P < 0.01$, Fig. 3 k). Finally, because PGE_2 is the final effector molecule on SMCs (downstream of astrocyte glycolysis), we could rescue vasodilation by applying PGE_2 in the presence of either oxamate (109.2 ± 2.2 %, $P < 005$, n = 5, Fig. 3 i) or IA (109.0 ± 1.3 %, $P < 0.01$, n = 5, Fig. 3 i). These data demonstrate that inhibition of glycolysis or LDH limits extracellular lactate and PGE_2 accumulation in response to t-ACPD in low O_2, preventing astrocyte mediated vasodilations.

As a final test of our hypothesis we pharmacologically targeted PGTs to manipulate extracellular levels of PGE_2 and examined the effects on vasomotion. First, blockade of PGTs with U46619[22] or TGBz T34[16] resulted in elevated levels of PGE_2 when mGluRs were activated in low O_2 (tACPD: 227.5 ± 7.2 %, tACPD + U46619: 435.6 ± 16.9, $P < 0.01$ to tACPD alone, n = 5; tACPD + T34: 816.4 ± 6.0, $P < 0.01$ to tACPD alone, n = 4, Fig. 4 a) and did not interfere with low O_2 astrocyte-mediated dilations (U46619: 110.4 ± 0.3 %, $P < 0.01$, n = 5; T34: 109.1 ± 1.3 %, $P < 0.01$, n = 7, Fig. 4 b). Second, we hypothesized that adding exogenous lactate in high O_2 would enable astrocyte-mediated vasomotion to change polarity by attenuating PGE_2 uptake. However, because there is nothing preventing the initiation of vasoconstriction in high O_2 from the action of AA in SMCs, we blocked constriction at the level of SMCs by adding adenosine[23]. Extracellular adenosine is elevated in a reduced oxygen environment[24] and is an additional modulator of vasoconstriction[23]. In the presence of adenosine (100 μM), uncaging Ca^{2+} within astrocytes in high O_2 produced no vasomotion (99.6 ± 0.9 %, $P > 0.05$, n = 4, Supplemental Fig. 4). However, when lactate (100 μM - 1 mM) was included to mitigate PGE_2 clearance in addition to adenosine, Ca^{2+} uncaging now resulted in dilation (107.5 ± 1.4 %, $P < 0.01$, n = 9, Fig. 4 b, c), despite equivalent endfeet Ca^{2+} signals compared to adenosine alone (adenosine: $F/F_0 = 160.4 ± 6.1$; adenosine + lactate: $F/F_0 = 159.6 ± 5.1$, $P > 0.05$, Supplemental Fig. 4). From this, we hypothesized that PGT blockade would have a similar result by raising the extracellular PGE_2 level. Indeed, in high O_2 we found that in the same vessel, the first uncaging event caused constriction (87.4 ± 1.8 %, $P < 0.01$, Fig. 4 b, d) but the second uncaging event during PGT inhibition with T34 caused dilation (108.7 ± 1.4 %, $P < 0.05$, n = 5, Fig. 4 b, d). These data indicate that the ability of astrocytes to induce dilation over constriction critically relies on reduced efficacy of PGE_2 uptake under conditions where lactate release is enhanced.

Here we show that when the glycolytic state of the brain is enhanced by lower O_2 levels, astrocyte-mediated vasoconstrictions convert to vasodilations because the elevated extracellular lactate causes PGE_2 accumulation which is maximized during mGluR activation. Flow through blood vessels is proportional to vessel radius to the 4^{th} power; therefore a ~9 % change in arteriole diameter reported here equates to a ~45 % increase in CBF. This change is consistent with astrocyte-mediated vasodilations observed *in vivo*[7] and can more than account for regional CBF changes measured by PET[25] and with two-photon microscopy[26] when the brain is physiologically activated. These data add an important and

until now unrecognized mechanism in the bidirectional control of cerebral vessels by astrocytes. Previous studies implicated different populations of GABA neurons[27] and tissue nitric oxide levels[2]. The metabolic control of these antagonistic pathways by astrocytes implies that brain blood flow would reach a homeostatic level depending on metabolic activity. Under quiescent periods when O_2 is not being rapidly consumed, astrocyte Ca^{2+} signals induce constrictor tone, keeping CBF at an appropriate level. At the onset of neural activity there is a drop in PO_2 and rise in extracellular lactate which promotes astrocyte mediated dilation. Manipulating this homeostatic balance may be a therapeutic avenue for treating the inappropriate declines in CBF that occurs in some dementias and after stroke.

Methods Summary

Brain Slices and Imaging

Hippocampal and neocortical slices were prepared from juvenile (p 16-21), male, Sprague-Dawley rats. Care and use of animals was approved by the University of British Columbia Animal Care and Use Committee. ACSF bubbled with 95 % O_2, 5 % CO_2 (standard for brain slice experimentation), was defined as a high O_2 treatment and ACSF bubbled with 20 % O_2, 5 % CO_2, balanced N_2, was defined as a low O_2 treatment. For astrocyte dye loading, slices were transferred to a 3 ml ACSF well containing the Ca^{2+} cage DMNPE-4/AM and/or the Ca^{2+} indicator rhod-2/AM dissolved in DMSO (final DMSO concentration 0.2 %) for 1.5 hours. A two-photon laser-scanning microscope (Zeiss LSM510-Axioskop-2 fitted with a 40X-W/0.80 numerical aperture objective lens) directly coupled to a Chameleon Ultra tunable ultrafast laser (~100-fs pulses and 76MHz, Coherent) provided excitation of rhod-2 intrinsic NADH fluorescence and was used for uncaging using two photon photolysis. Arterioles were identified with IR-DIC optics and vessel diameter changes were imaged by acquiring the transmitted laser light. Quantification of lumen diameter, NADH and Ca^{2+} changes were performed with Zeiss LSM (version 3.2) software and ImageJ.

Lactate and PGE_2 Measurements

The assay used for measuring PGE_2 release was Specific Parameter PGE_2 ELISA kits (R&D systems). Extracellular lactate levels were measured using a Lactate Assay Kit (Biomedical Research Service Centre, SUNY Buffalo).

Full Methods and associated references can be found below in the supplemental materials section.

Supplementary Material

Refer to Web version on PubMed Central for supplementary material.

Acknowledgments

We thank Drs. T. Murphy, Tony Phillips and Yu Tian Wang for reading an earlier version of the manuscript. T34 was a gift from the lab of Victor L. Schuster from the Departments of Medicine and Physiology and Biophysics, Albert Einstein College of Medicine. Supported by an operating Grant from the Canadian Institutes of Health Research. BAM is a Canada Research Chair and a Michael Smith Foundation for Health Research (MSFHR) Distinguished Scholar. GRJG is supported by fellowships from the Alberta Heritage Foundation for Medical

Research and MSFHR. HBC is supported by postdoctoral fellowships from Wilms Foundation and the Heart and Stroke Foundation of BC and the Yukon.

References

1. Mulligan SJ, MacVicar BA. Calcium transients in astrocyte endfeet cause cerebrovascular constrictions. Nature. 2004; 431(7005):195. [PubMed: 15356633]
2. Metea MR, Newman EA. Glial cells dilate and constrict blood vessels: a mechanism of neurovascular coupling. J Neurosci. 2006; 26(11):2862. [PubMed: 16540563]
3. Chuquet J, Hollender L, Nimchinsky EA. High-resolution in vivo imaging of the neurovascular unit during spreading depression. J Neurosci. 2007; 27(15):4036. [PubMed: 17428981]
4. Zonta M, Angulo MC, Gobbo S, et al. Neuron-to-astrocyte signaling is central to the dynamic control of brain microcirculation. Nature neuroscience. 2003; 6(1):43.
5. Filosa JA, Bonev AD, Nelson MT. Calcium dynamics in cortical astrocytes and arterioles during neurovascular coupling. Circulation research. 2004; 95(10):e73. [PubMed: 15499024]
6. Filosa JA, Bonev AD, Straub SV, et al. Local potassium signaling couples neuronal activity to vasodilation in the brain. Nature neuroscience. 2006; 9(11):1397.
7. Takano T, Tian GF, Peng W, et al. Astrocyte-mediated control of cerebral blood flow. Nature neuroscience. 2006; 9(2):260.
8. Ido Y, Chang K, Williamson JR. NADH augments blood flow in physiologically activated retina and visual cortex. Proceedings of the National Academy of Sciences of the United States of America. 2004; 101(2):653. [PubMed: 14704275]
9. Mintun MA, Vlassenko AG, Rundle MM, et al. Increased lactate/pyruvate ratio augments blood flow in physiologically activated human brain. Proceedings of the National Academy of Sciences of the United States of America. 2004; 101(2):659. [PubMed: 14704276]
10. Vlassenko AG, Rundle MM, Raichle ME, et al. Regulation of blood flow in activated human brain by cytosolic NADH/NAD+ ratio. Proceedings of the National Academy of Sciences of the United States of America. 2006; 103(6):1964. [PubMed: 16446430]
11. Ances BM, Buerk DG, Greenberg JH, et al. Temporal dynamics of the partial pressure of brain tissue oxygen during functional forepaw stimulation in rats. Neuroscience letters. 2001; 306(1-2): 106. [PubMed: 11403969]
12. Offenhauser N, Thomsen K, Caesar K, et al. Activity-induced tissue oxygenation changes in rat cerebellar cortex: interplay of postsynaptic activation and blood flow. The Journal of physiology. 2005; 565(Pt 1):279. [PubMed: 15774524]
13. Vanzetta I, Grinvald A. Increased cortical oxidative metabolism due to sensory stimulation: implications for functional brain imaging. Science (New York, NY. 1999; 286(5444):1555.
14. Devor A, Ulbert I, Dunn AK, et al. Coupling of the cortical hemodynamic response to cortical and thalamic neuronal activity. Proceedings of the National Academy of Sciences of the United States of America. 2005; 102(10):3822. [PubMed: 15734797]
15. Ellis-Davies GC. Caged compounds: photorelease technology for control of cellular chemistry and physiology. Nature methods. 2007; 4(8):619. [PubMed: 17664946]
16. Chi Y, Khersonsky SM, Chang YT, et al. Identification of a new class of prostaglandin transporter inhibitors and characterization of their biological effects on prostaglandin E2 transport. The Journal of pharmacology and experimental therapeutics. 2006; 316(3):1346. [PubMed: 16269530]
17. Chan BS, Endo S, Kanai N, et al. Identification of lactate as a driving force for prostanoid transport by prostaglandin transporter PGT. Am J Physiol Renal Physiol. 2002; 282(6):F1097. [PubMed: 11997326]
18. Hu Y, Wilson GS. A temporary local energy pool coupled to neuronal activity: fluctuations of extracellular lactate levels in rat brain monitored with rapid-response enzyme-based sensor. Journal of neurochemistry. 1997; 69(4):1484. [PubMed: 9326277]
19. Kasischke KA, Vishwasrao HD, Fisher PJ, et al. Neural activity triggers neuronal oxidative metabolism followed by astrocytic glycolysis. Science (New York, NY. 2004; 305(5680):99.
20. Nimmerjahn A, Kirchhoff F, Kerr JN, et al. Sulforhodamine 101 as a specific marker of astroglia in the neocortex in vivo. Nature methods. 2004; 1(1):31. [PubMed: 15782150]

21. Brown AM, Ransom BR. Astrocyte glycogen and brain energy metabolism. Glia. 2007; 55(12): 1263. [PubMed: 17659525]

22. Pucci ML, Endo S, Nomura T, et al. Coordinate control of prostaglandin E2 synthesis and uptake by hyperosmolarity in renal medullary interstitial cells. Am J Physiol Renal Physiol. 2006; 290(3):F641. [PubMed: 16263809]

23. Bryan, RM, Jr. Cerebral Blood Flow and Metabolism. Edvinson, L.; Krause, DN., editors. Lippincott Williams and Wilkins; Philadelphia: 2002. p. 311

24. Frenguelli BG, Llaudet E, Dale N. High-resolution real-time recording with microelectrode biosensors reveals novel aspects of adenosine release during hypoxia in rat hippocampal slices. Journal of neurochemistry. 2003; 86(6):1506. [PubMed: 12950459]

25. Fox PT, Raichle ME. Stimulus rate dependence of regional cerebral blood flow in human striate cortex, demonstrated by positron emission tomography. Journal of neurophysiology. 1984; 51(5): 1109. [PubMed: 6610024]

26. Chaigneau E, Tiret P, Lecoq J, et al. The relationship between blood flow and neuronal activity in the rodent olfactory bulb. J Neurosci. 2007; 27(24):6452. [PubMed: 17567806]

27. Cauli B, Tong XK, Rancillac A, et al. Cortical GABA interneurons in neurovascular coupling: relays for subcortical vasoactive pathways. J Neurosci. 2004; 24(41):8940. [PubMed: 15483113]

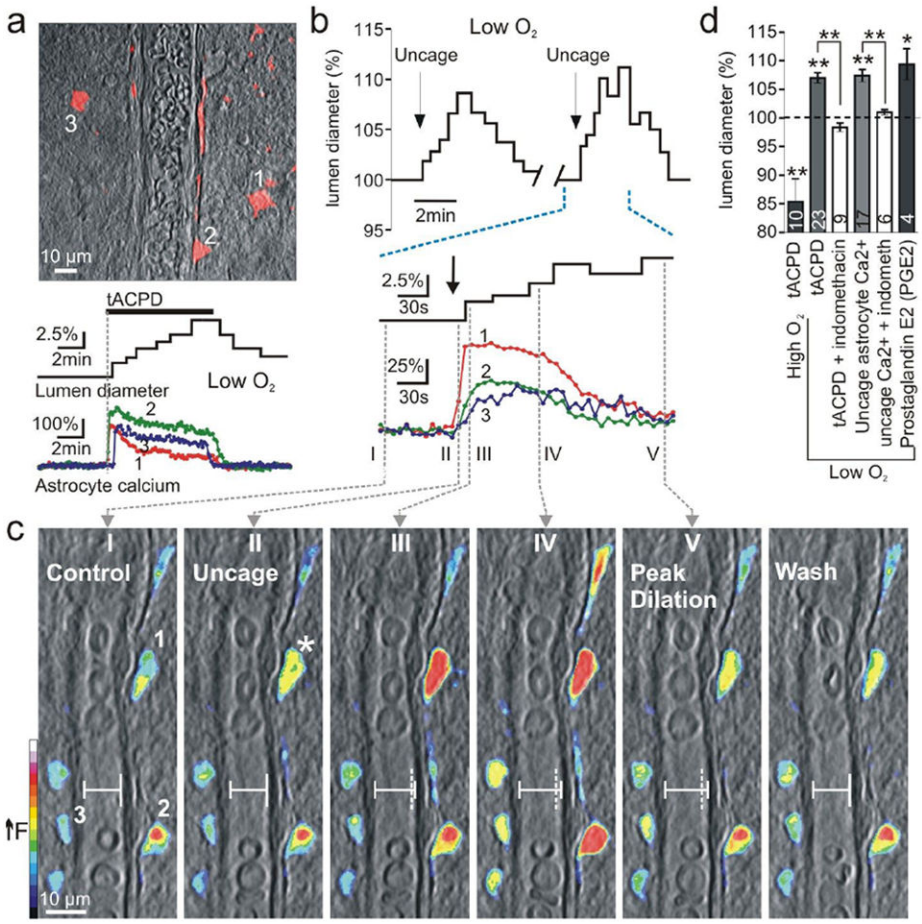

Fig. 1.

Lowering O_2 converts astrocyte-mediated vasoconstrictions to vasodilations. (a) Top: astrocytes (red) loaded with Ca^{2+} indicator surround arteriole. Bottom: astrocyte Ca^{2+} signals occur coincident with dilation caused by the mGluR agonist t-ACPD in low O_2. (b) Top: uncaging astrocyte Ca^{2+} (indicated by arrow) causes vasodilation in low O_2 and is repeatable. Bottom: expanded time scale shows the Ca^{2+} signal in endfoot 1 (shown in *c I*) precedes the lumen diameter increase. (c) Overlay of vessel and pseudo colored endfoot Ca^{2+} changes. Images *I*-*V* correspond to times in *b*. *I*: control state and regions of interest: endfeet 1-3. Image *II*: endfoot 1 shows first Ca^{2+} rise (star) before lumen diameter starts to increase. Vertical dotted line (*III*-*V*) indicates previous position of vessel wall. (d) Summary data.

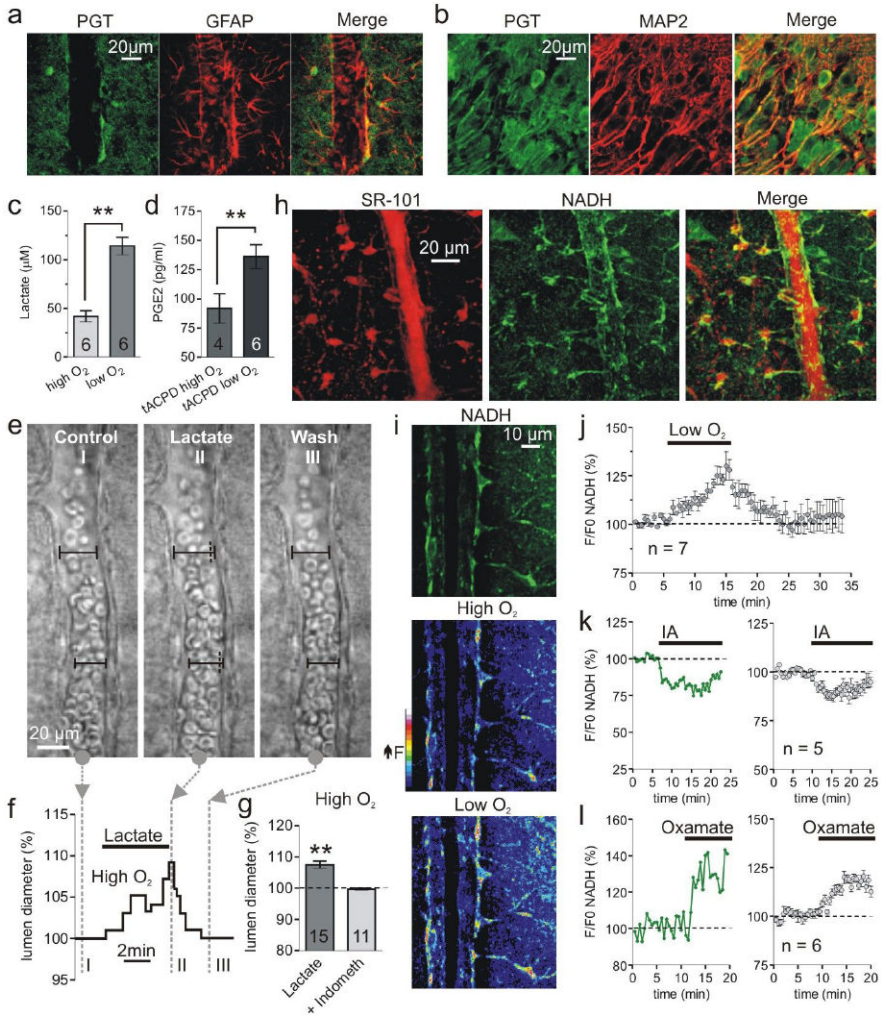

Fig. 2.

Low O_2 facilitates lactate and PGE_2 release and enhances astrocyte glycolysis. (a and b) Immunohistochemistry showing the astrocyte marker GFAP and the neuron marker MAP2 colocalize with PGT labeling. (c) Lactate release is elevated in low O_2. (d) t-APCD increases PGE_2 release most in low O_2. (e and f) Lactate dilates an arteriole. Images *I-III* correspond to time points in *f*, which shows the lumen diameter increase. (g) Summary showing percent dilation by lactate and block by indomethacin. (h) Colocalization of the astrocyte maker SR-101 (left stack) and the NADH signal (middle stack) from perivascular glia somas and endfeet. (i) Top: arteriole NADH fluorescence from a single image plane showing astrocyte compartments, SMCs/endothelial cells and empty lumen of the blood vessel. Middle and Lower: pseudo colored image of NADH fluorescence in high and low O_2. (j) Summary of NADH changes in astrocyte compartments caused by low O_2. (k and l) Astrocyte NADH in response to glycolysis inhibition with iodoacetate (IA) (k) and LDH inhibition with Oxamate (l). Left: single experiment; right: summary.

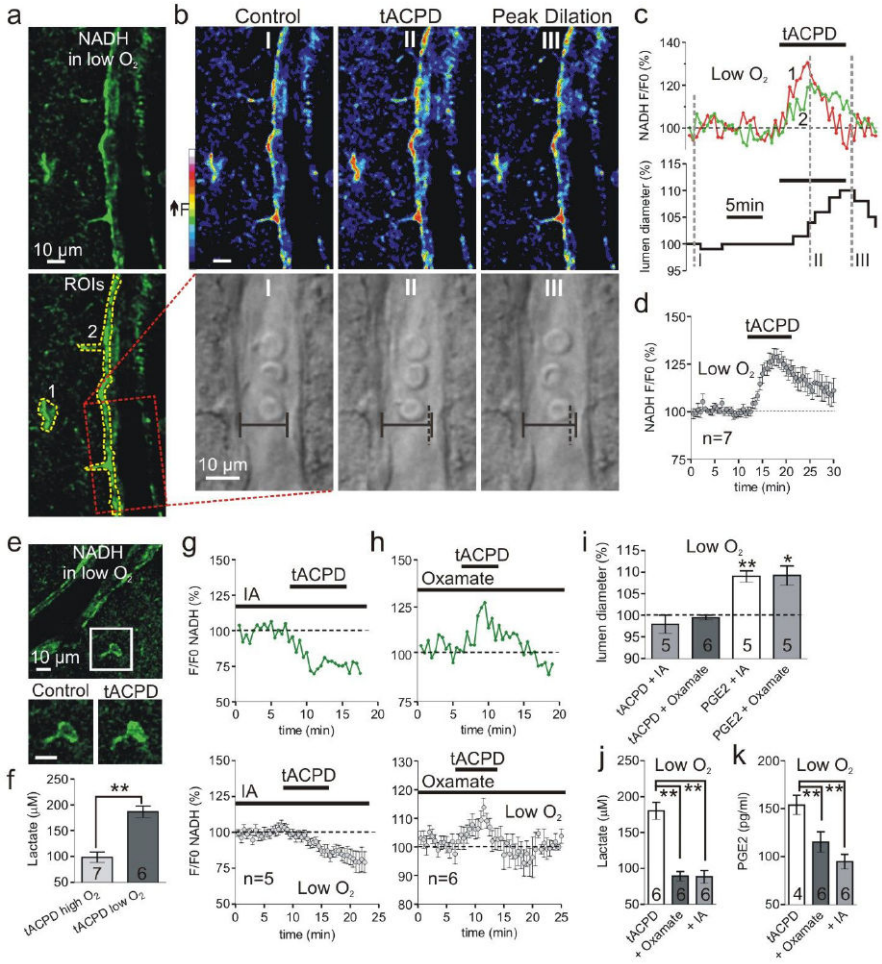

Fig. 3.

Glycolysis and lactate release is critical for astrocyte-mediated dilations. (a) Arteriole and astrocyte NADH image in low O_2; bottom shows ROIs for astrocyte compartments (1 and 2) and vessel (box). (b) Pseudo color NADH (top) and diameter (bottom) changes caused by t-ACPD at time points *I-III* in *c*. Vertical dotted line (*II* and *III*) indicates previous position of vessel wall. (c) Astrocyte NADH (top) and lumen diameter (bottom) in response to t-ACPD; same experiment as *a* and *b*. (d) Summary of NADH increase from mGluR activation in low O_2. (e) Top: NADH image of an arteriole and astrocyte. Lower: soma close-up showing t-ACPD causes a diffuse increase in NADH. (f) t-ACPD increases extracellular lactate most in low O_2. (g) t-ACPD decreases astrocyte NADH during glycolysis inhibition; top: single experiment; bottom: summary. (h) mGluR activation increases astrocyte NADH during LDH inhibition; top: single experiment; bottom: summary. (i) Summary showing t-ACPD fails to dilate vessels in oxamate or IA and PGE_2 rescues vasodilation in these compounds. (j and k) The increase in lactate (j) and PGE_2 (k) caused by t-ACPD is significantly less in oxamate and IA.

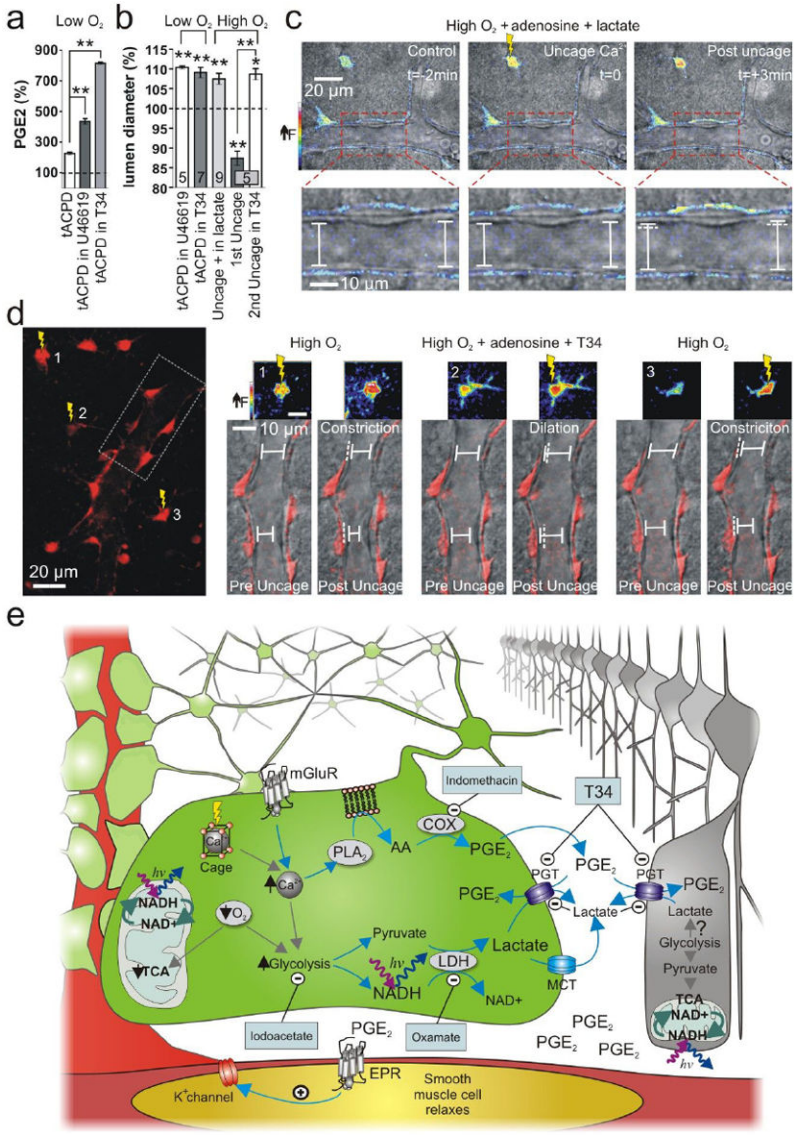

Fig. 4.

Raising PGE_2 levels by inhibiting PGT changes the polarity of astrocyte-mediating vasomotion. (a) PGE_2 levels were further elevated by mGluR activation in low O_2 when PGT was inhibited by U46619 or T34. (b) Summary data of vasomotion during PGT manipulation. (c) Uncaging Ca^{2+} in high O_2 causes vasodilation in exogenous lactate. Top panels show the astrocyte Ca^{2+} signal change (pseudo colour) from uncaging. Lower panels show close up of vessel lumen. (d) In high O_2, astrocyte-mediated vasoconstriction is converted to vasodilation during PGT blockade. Left: astrocytes and endfeet circumscribing an arteriole. Ca^{2+} is uncaged in 3 astrocytes separated in time; box indicates the vessel region examined on the right. Right: vasomotions corresponding to the separate uncaging events. Small pseudo colour images show the Ca^{2+} signal change from uncaging in each astrocyte. Lower images of the vessel and endfeet (red) show that the vasomotion switches polarity when PGTs are blocked. (e) Diagram of the supported model.